

Electrochemistry of active chromium. Part IV. Dissolution of chromium in deaerated sulfuric acid

D. M. DRAŽIĆ^{1*#}, J. P. POPIĆ^{1#}, B. JEGDIĆ² and D. VASILJEVIĆ-RADOVIĆ³

¹ICTM-Center for Electrochemistry, Njegoševa 12, P. O. Box 473, 11001 Belgrade (e-mail: dmdrazic@eunet.yu), ²Technical Military Institute, Katanićeva 14, 11000 Belgrade and ³ICTM-Center for Microelectronic Technologies and Single Crystals, Njegoševa 12, P. O. Box 473, 11001 Belgrade, Serbia and Montenegro

(Received 28 May 2004)

Abstract: Chromium dissolution in aqueous sulfuric acid solutions in the pH range 0.5–3 was studied electrochemically by the potentiostatic or very slow potentiodynamic method, and by the analyses of the Cr ion concentrations in the electrolyte formed during the experiments. It was shown that the electrochemical anodic dissolution follows a common Tafel line with a slope of *ca.* 120 mV dec⁻¹, independent of the solution pH and the hydrodynamics, while the passivation potentials and passivation currents were independent on hydrodynamics but strongly dependent on the pH. In parallel with the electrochemical dissolution, a considerable “anomalous” or chemical Cr dissolution process occurs, as evidenced by the spectrophotometric analyses of the electrolytes for Cr ions after prolonged potentiostating of the electrodes at different potentials, as well as by measuring the electrode weight losses. All these results indicate the existence of a potential independent reaction of Cr dissolution occurring in parallel to the anodic dissolution process. Mechanisms for both the electrochemical and the chemical process are proposed. The consequences of these phenomena on the behavior of some practical systems where chromium or a chromium alloy (*e.g.*, stainless steels) are used are discussed.

Keywords: chromium, acid solutions, anodic dissolution, anomalous dissolution, chemical dissolution, reaction mechanisms.

INTRODUCTION

The corrosion stability and electroplating properties of Cr when used either as protective or decorative coatings, or, as a dominant component of stainless steels is certainly dependent on the kinetics of the electrochemical dissolution of Cr and accompanying phenomena. The good protective properties of Cr coatings are due to the ease with which Cr reacts with O₂ from air with the formation of a stable pas-

* Author for correspondence.

Serbian Chemical Society active member.

sive film. This film, however, can be easily removed either by cathodic polarization with hydrogen evolution,¹ or by mechanical action on Cr,² or stainless steel surface. This might happen also inside the cracks, which form during the action of force on stainless steel parts, causing damages due to corrosion fatigue or even stress corrosion cracking.

The purpose of this communication is to shed more light onto the rather contradictory interpretations of the anodic dissolution processes in the active potential dissolution range, and to separate in a quantitative way the contribution of the electrochemical process, its kinetics and reaction products, from a parallel “anomalous” (chemical) dissolution process which occurs at a considerable rate.^{1,3,4}

EXPERIMENTAL

The experiments were performed with metallic Cr (Merck, lumps). The electrodes were made either in the form of a piece of metal sealed in epoxy resin (exposed surface 2 cm²) or as a Cr disc inserted into the metal disc of a PINE rotating system. PINE potentiostat RDE 4 and a two-channel Philips X-Y plotter were used. All the experiments were performed in aqueous mixtures of 0.1 M Na₂SO₄ + H₂SO₄ (pH 0.5 – 3). Merck p.a. chemicals and doubly distilled water were used for the preparation of the solutions. An all-glass three compartment electrochemical cell with a Pt foil as the counter electrode and a saturated calomel reference electrode (SCE) was used. All the potentials are referred to SCE. The solutions were continuously deaerated with purified nitrogen.¹ The experiments were carried out at ambient temperature (22 ± 2 °C). The potential scan rate of the Cr electrode was 2 mV s⁻¹, which appeared to be sufficiently slow to consider the polarization curves to have been obtained under quasi-steady state condition. Prior to the measurements, the electrodes were activated by cathodic polarization at – 0.9 V for 90 s, since the spontaneously formed open circuit potential of an electrode which had previously been in contact with air was about –0.450 V, which corresponds to the passive state of the chromium surface.

For the determination of chromium ion concentration by means of a Hewlett-Packard HP8452A spectrophotometer a quartz cell with a stopper was used in order to eliminate the possibility of oxidation of Cr(II) ions by air oxygen. Also, care was taken when removing the samples from the cell, which had a stopcock at the bottom for passing the solution samples directly into the quartz cell. Details on the difficulties involved in the spectrophotometry of Cr(II) ions and mixtures of Cr(II) and Cr(III) ions have been presented elsewhere.¹

The crystalline structure of the electrode sample was studied by optical microscopy and by back scattering X-ray diffracton. A Unicam-Cambridge S.25 goniometer for monocrystals with Philips PW generator with copper anticathode (λ CuK α_1 , 40 kV, 20 mA) was used. Morphology of the surface after corrosion or anodic polarization was observed using optical microscopy, scanning electronic microscopy (SEM) (Jeol T20) and atomic force microscopy (AFM) techniques (AFM-Autoprobe CP Research, Thermomicroscopes, Ca, USA).

RESULTS

Figure 1 depicts typical polarization curves for chromium in acid solutions (aqueous Na₂SO₄ + H₂SO₄, pH 0.5 – 3), in this case for pH 1. The corrosion potential $E_{\text{corr},1}$ obtained directly after the introduction of Cr electrode into the electrolyte was in the range of – 0.400 V, while after cathodic pretreatment and activation of the Cr surface, $E_{\text{corr},2}$ was in the range – 0.680 to – 0.840 mV, which means that the corrosion potential, $E_{\text{corr},2}$, changes by about – 60 mV/pH (see Ref. 3). In the same diagram the filled squares represent the spectrophotometric (analytic) data

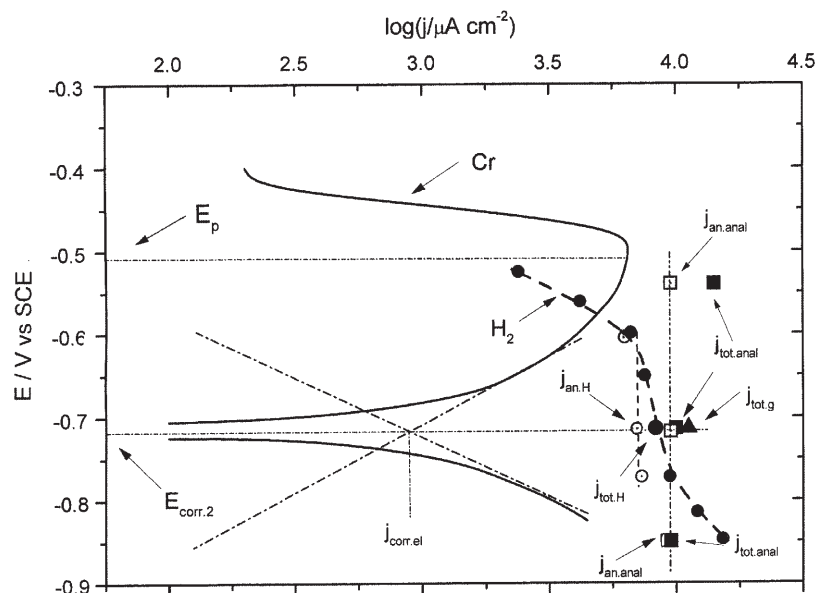


Fig. 1. Anodic and cathodic polarization curves and corrosion potential for an activated ($E_{\text{corr},2}$) Cr electrode at pH 1.0. (0.5 M $\text{Na}_2\text{SO}_4 + \text{H}_2\text{SO}_4$), (—) H_2 evolution rates on active Cr calculated from volumetric data. (---) Partial anodic and cathodic Tafel lines. Total corrosion current densities determined: (●)-volumetrically, (▲)-gravimetrically and (■)-analytically. Electrochemical corrosion current density $-j_{\text{corr},\text{el}}$. The anomalous dissolution current densities (vertical dash and double dots line) are the differences between the total and the electrochemical corrosion current densities. (□ – calculated from analytical; ○ – from volumetric data). Sweep rate 2 mV s^{-1} .

recalculated into the equivalent $j_{\text{tot},\text{anal}}$. Besides, at the corrosion potential, *i.e.*, for the corrosion rate, analytical data were also obtained, for the cathodically and anodically polarized electrode. After correction of the analytically obtained data for the simultaneous anodic dissolution current, the corrected $j_{\text{an},\text{anal}}$, *i.e.*, “anomalous” dissolution rates (open squares) were obtained. These points lie on a vertical (double dot dash) line, indicating the *independence* of the dissolution process *on potential*. In a solution of pH 1, this process is rather fast, and is *ca.* 10 times faster than the electrochemical corrosion rate, $j_{\text{corr},\text{el}}$.

Superimposed polarization diagrams for three different pH values, 1, 2 and 3, are presented in Fig. 2. As can be seen, the cathodic Tafel lines for H_2 evolution are shifted, as expected, for by the discharge of H_3O^+ ions, while the anodic Tafel lines are rather short, but all lie on the *same line* with an anodic slope of *ca.* 120 mV dec^{-1} . This also shows that the anodic reaction *does not* depend on pH, the positions of the experimental anodic lines being determined by the pH dependence of the cathodic Tafel lines and the pH dependence of the passivation potentials. The experiments with the rotating Cr disc electrode revealed that the passivation currents did not depend on the rotation speed, while the passivation potential depended on pH, $dE_p/d\text{pH} \approx 100 \text{ mV}$.

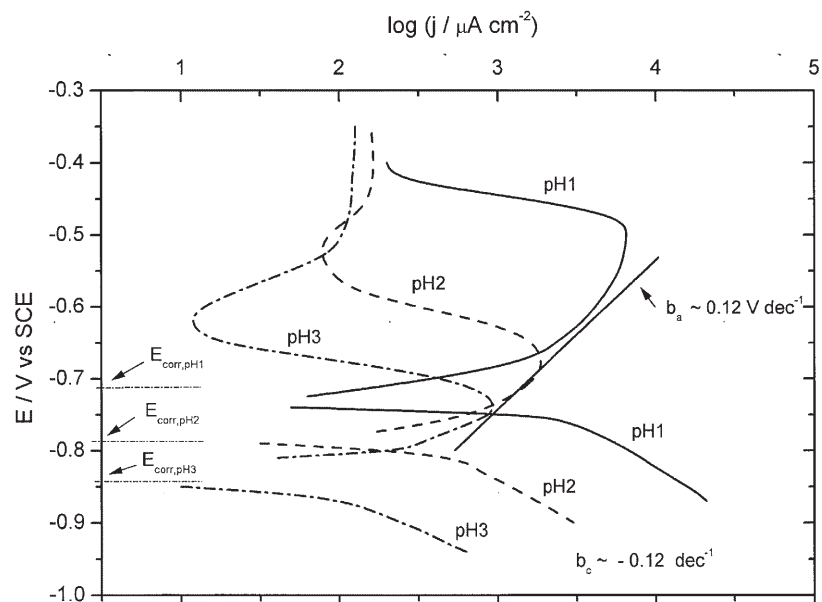


Fig. 2. Cathodic and anodic polarization curves for three different pH values: 1, 2 and 3.

Figure 3 depicts the dependence of the “anomalous” dissolution reaction on pH, showing a slope of -0.89 . Bearing in mind the possible experimental errors in determining the values, it can be interpreted as that the reaction order of this reac-

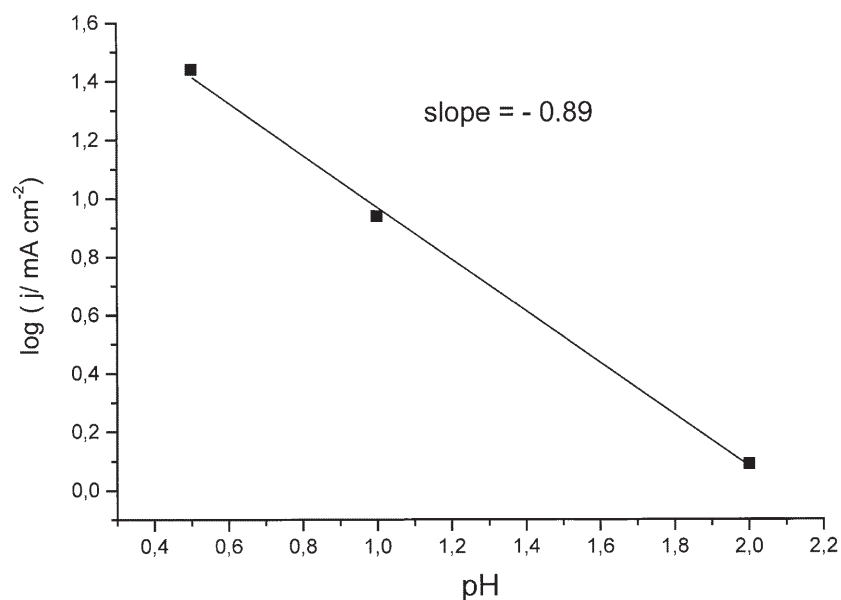


Fig. 3. Dependence of the logarithm of the rate (expressed as the equivalent current density, $j_{\text{an,anal}}$) of the “anomalous” chromium dissolution reaction on pH.

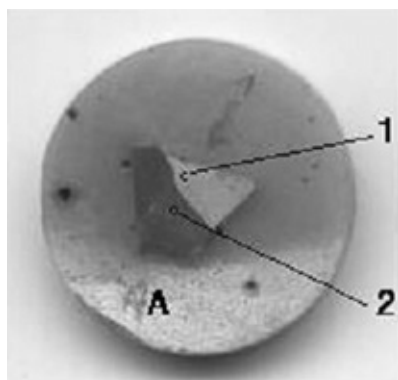


Fig. 4. Photograph of the electrode specimen used in the electrochemical and structural investigation. After etching in sulfuric acid, two distinct surfaces appeared, marked with 1 and 2. A designates the epoxy holder.

tion regarding H_3O^+ ions is practically 1, and that the “anomalous” dissolution rate decreases with increasing pH in the range studied. In an experiment at pH 1, the Na_2SO_4 concentration was increased from 0.1 M to 1.0 M, but the “anomalous” dissolution rate was not affected, *i.e.*, sulfate ions do not participate in the “anomalous” process.

The chromium electrode used in these experiments was sealed in epoxy resin and the microphotograph of it is shown in Fig. 4. After fine polishing and etching (for 120 min at the open circuit potential after cathodic activation), the microphotograph shows two large more or less homogeneous surfaces, marked with the numbers 1 and 2. A in Fig. 4 marks the epoxy holder. It is obvious that the electrode material at the surface exposed to the electrolyte consists practically of two large separate crystals, marked as surface 1 and surface 2. The lauegram presented in Fig. 5a does not show any reflection even after 8 h of exposure, while Fig. 5b represents the result of a 2 h exposure of the surface 2 under the same angle. Except the network of points, this diffracton photograph shows a very intensive reflection under an angle of 22° . Therefore, it can be concluded that the part of the electrode marked by 2 represents the single crystal structure of the body-centered cubic lattice of chromium with an interlayer distance of 0.83 \AA , which according to the data for chromium card in card catalog JSPDS No. 06-0694, corresponds to the Miller

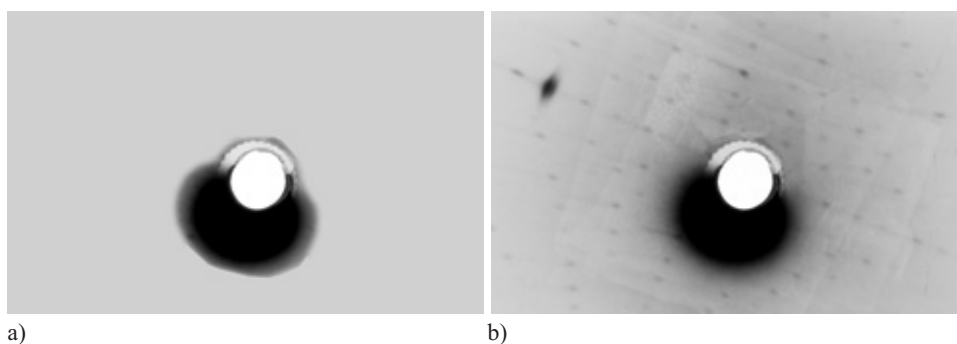


Fig. 5. Lauegrams of: (a) surface 1; (b) surface 2.

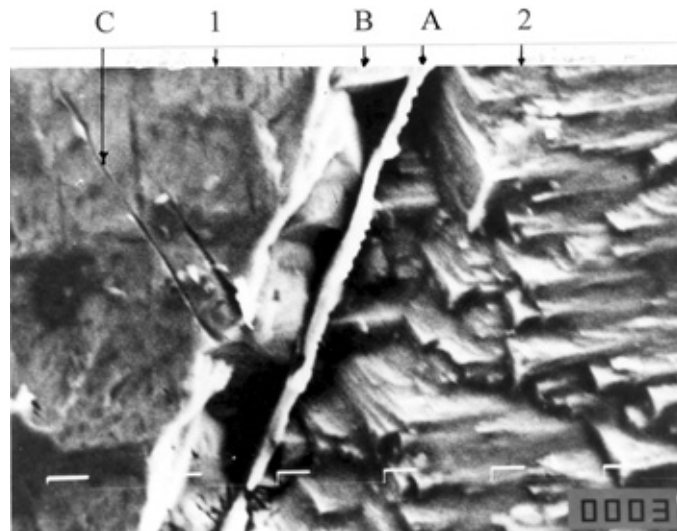


Fig. 6. SEM Micrograph of the electrode at the boundary between surfaces 1 and 2.

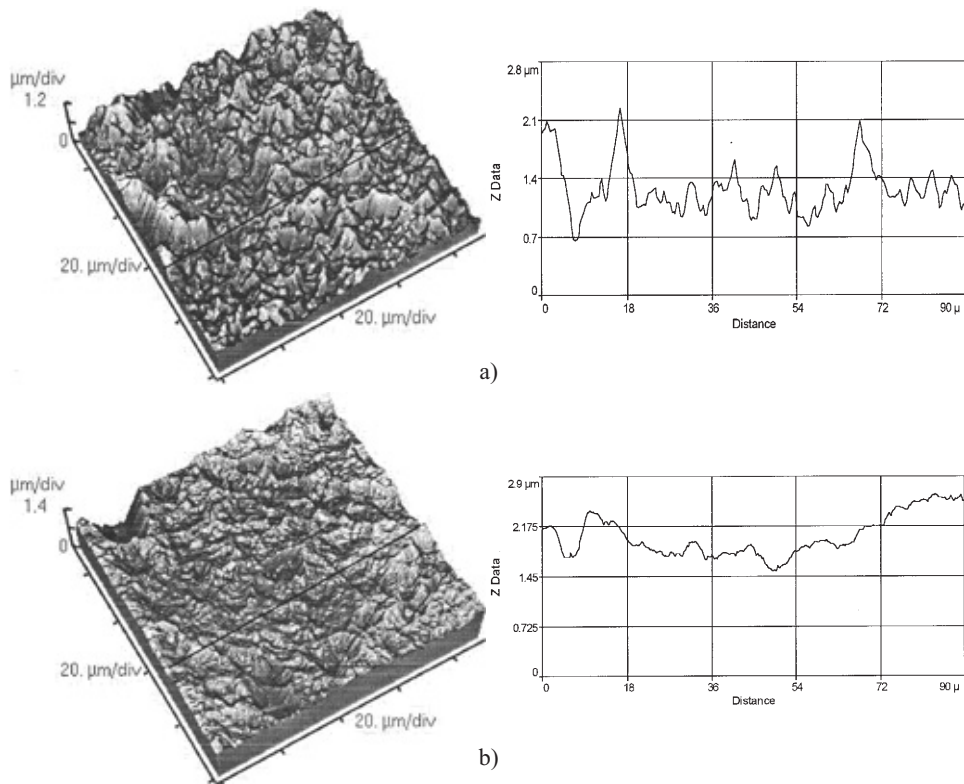


Fig. 7. Atomic force microscopy (AFM) images of: (a) surface 1, (b) surface 2. Black lines indicate the tip moving tracks. Diagrams represent the tip oscillation along the tracks.

indices (222) positioned under 22° towards the electrode surface exposed to the electrolyte. On the other hand, lauegram in Fig. 5a shows no reflections, which allows, with a great probability, the conclusion that the part of the electrode marked 1 has no crystalline structure.

Figure 6 is the SEM microphotograph of the electrode surface after etching (the same as for Fig. 4) at the position of the boundary between the two large crystals at a magnification of 2000. The right-hand side belongs to the crystal marked with 2 in Fig. 4, and a rough crystalline surface characteristic for the cubic lattice is seen after the etching. The left-hand side of the same microphotograph shows a quite different morphology of a more amorphous character at this level of magnification of the surface marked with 1 in Fig. 4. Three interesting features should be noticed here: a thin white boundary between surfaces 1 and 2 (marked with A), a deep narrow channel right behind the boundary layer (B), and long thin cracks (C) of considerable length on a part of surface 1, not visible on a part 2.

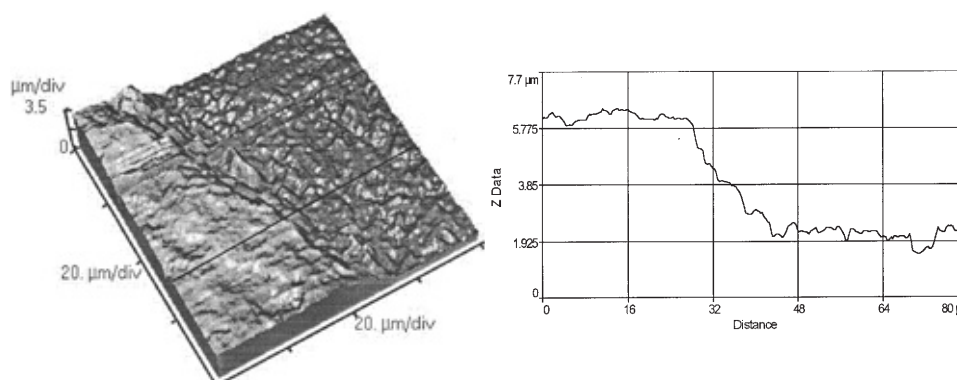


Fig. 8. AFM image of the boundary between the surfaces 1 and 2. Black line indicates the tip moving track.

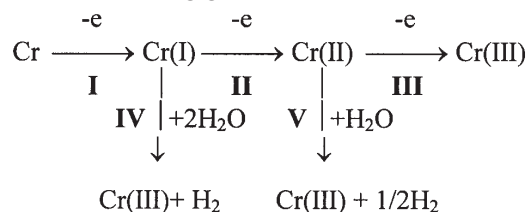
AFM images obtained with the same electrode specimen are shown in Figs. 7a for surface 1, and 7b, for the surface 2. It is obvious that surface 1 is rougher than surface 2. This can be seen in a more quantitative manner in Fig. 8 when an image of the surface at the boundary was made and the standard roughnesses of both surfaces are graphically and numerically presented. The average roughness R_a of the surface 1 is $0.218 \mu\text{m}$, which is about 1.4 times rougher surface than surface 2 ($R_a = 0.156 \mu\text{m}$).

The second, more important conclusion from the surface image shown in Fig. 8 is that the rate of anodic dissolution is different for the different surfaces. For the same dissolution time, the level of the surface 1 became about $2 \mu\text{m}$ deeper than the level of the surface 2, indicating different rates of the anodic reaction at these two different surfaces.

DISCUSSION

Anodic dissolution process

It was shown elsewhere¹ that the reaction products of the corrosion and anodic dissolution of Cr are Cr(II) and Cr(III) ions in the ratio of *ca.* 7:1; independently of the potential. Hence, the following general reaction scheme can be considered



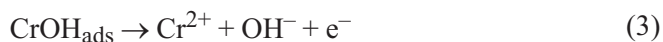
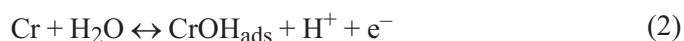
Scheme 1.

Bearing in mind the experimentally obtained anodic Tafel slope which can be considered to correspond to a value of 120 mV dec^{-1} , the theoretically expected are for a single electron charge exchange step, and the independence of the rate on pH, *three reaction schemes* can be proposed:

(i). The sequence **I**, **II** and 1/8 of the product by **III**, with step **I** being the rate determining one (rds). Reactions **IV** and **V** are not of importance since, as experimentally proved the anodic co-evolution of H_2 does not depend on anodic polarization.³ According to the mechanism, the rates of reactions **IV** and **V** would be expected to increase as the anodic current and polarization increase, since the surface concentration of the intermediates Cr(I) and Cr(II) should increase with increasing anodic polarization. As was seen, this is not the case.

(ii). The sequence **I**, **II** and 1/8 of the product by **III**, with step **II** as the rds, if the surface coverage of adsorbed Cr(I) is large ($\theta \rightarrow 1$).

(iii). The following scheme could be considered bearing in mind the great interaction of Cr with H_2O (as is the case with Fe, Ni and Co⁵):



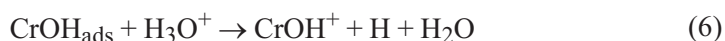
in which the second step is the rds and the surface coverage with CrOH_{ads} is large ($\theta \rightarrow 1$). This is similar to the mechanism proposed for the anodic dissolution of Fe.⁶ The change of the corrosion potential with pH of $dE_{\text{corr},2}/d\text{pH} \approx -60 \text{ mV/pH}$ is in accordance with the proposed anodic dissolution mechanism and the hydrogen evolution reaction occurring by the discharge of H^+ ions as proposed in Part II of this series.⁴ This also confirms that the effective corrosion potential $E_{\text{corr},2}$ is a true electrochemically controlled value, in accordance with the Wagner-Traud model of electrochemical corrosion.⁸

It should be pointed out here that this similarity of the two mentioned reaction mechanisms is not unexpected, bearing in mind that the interaction of metals with water molecules increases as the position of the metal in the Volta line becomes more negative. This is obvious in the case of alkali and alkaline earth metals which readily react with water and which are very electronegative, as is well known. Also Al and Ti, known for their high reactivity with oxygen from the air and water molecules belong here, as well. All of them are very electronegative metals, having experimentally unmeasurable equilibrium potentials in aqueous solutions. Chromium with an equilibrium potential of $E_r^0 = -0.913$ V (SHE) (or -1.155 V (SCE))⁷ is much more negative than the members of the iron groups of metals, and hence the expected interaction with water or oxygen should be more intensive. The case of chromium is rather interesting since more negative elements, such as Al or Ti, are typical so-called valve metals, having oxide film which conducts electronically only in one direction, and are electrochemically irreducible. Chromium as a less electronegative metal behaves as a passive, or a valve metal when introduced into the electrolyte after previously being in contact with air, and exhibits a stable corrosion potential, $E_{\text{corr},1}$, in the range of -0.4 to -0.5 V. As in the case of Al, this is a mixed potential of the Wagner–Traud type⁸ with the cathodic hydrogen evolution reaction occurring on the oxide covered surface (see Ref. 4). However, after cathodic polarization to about -0.9 V for some time (see Experimental), the surface of chromium starts behaving as an electrochemically active metal with a second stable corrosion potential, $E_{\text{corr},2}$ in the range of -0.7 to -0.85 V, depending on the pH of the solution. Such a dual electrochemical behavior is not common for other electrode materials. Also, the pH dependence of the passivation potential, E_p , indicates that the passive layer formed during the passivation process includes OH groups, in some way, into the passive layer formed during the anodic reaction.⁴ The independence of the passivation current densities on the rotation speed of the rotating disc electrodes indicates that the mechanism of the passivation process is not of the dissolution-precipitation type but rather of a direct surface reaction.

“Anomalous” dissolution process

Our experimental results support the mechanism of the “anomalous” dissolution of metals proposed by Kolotyrkin and coworkers^{9–16} who observed that for a number of metals such as Fe, Ni, *etc.*, an “anomalous” dissolution process occurs, which is independent of the potential when the overall dissolution rate was measured by increasing the metal ion concentration during the change of cathodic polarization. They assumed that this process proceeds as a simple chemical reaction of metal atoms from the surface of a solid phase and water molecules adjacent to the surface of the metal in contact with the aqueous electrolyte. Hence, they termed this reaction also “chemical” pointing that there is no electron exchange between the metal and species reacting within the double layer, which is present, should

obey the laws of electrochemical kinetics (*i.e.*, the process should be potential dependent). It should also be mentioned that recently one of the authors of this series of papers proposed a new term “electroless” for this type of reaction¹⁵ in an attempt to stress the difference between the electrochemical dissolution processes and the observed “anomalous” behavior. However, it turned out, that this was an unfortunate translator’s mistake, but it certainly did not help the already existing ignorance in the Anglo-Saxon literature [*e.g.*, Ref. 17] for Kolotyrkin’s view on the possibility of a chemical explanation for the “anomalous” behavior of a number of important metals. It should also be pointed out than in some cases Kolotyrkin and coworkers observed that for some metals (*e.g.*, Cr and Fe¹⁴), the chemical reaction was pH dependent with and approximate reaction order regarding H₃O⁺ ions of 1 or 0.5. Bearing all this in mind, we propose the following reaction mechanism for the chemical dissolution process



with the second step being the rds, and probably with a large surface coverage with CrOH_{ads} ($\theta \rightarrow 1$). It has the *same first step* as the electrochemical reaction (reaction (2)).

Electrodes structure and morphology analysis

X-Ray analysis, shown in Figs. 5a and b, revealed that the part of the electrode marked with 2 (Fig. 5b) showed Laue patterns belonging to a single crystal structure of a bcc crystal of Cr. Contrary to this, the surface 1 (Fig. 5a) did not show any indication of a crystalline structure even after a rather long exposure time (8 h), hence it may be concluded that this part of the electrode did not have sufficient time to crystallize during cooling and remained in a more or less amorphous or subcrystalline state. This difference in the structure of the two surfaces can also be seen on the SEM microphotograph shown in Fig. 6. Surface 2 shows clear crystalline etching patterns, corresponding to the cubic crystalline system of chromium. This cannot be seen for surface 1. The boundary layer A in Fig. 6 consists of chromium sulfide as was shown by EDEX analysis, which obviously appeared as the result of a precipitation reaction of Cr with a small amount of impurities in the bulk of the crystal. The deep channels B appearing behind the sulfide boundary layer on surface 1 are of interest. The increased dissolution rate at these places close to the sulfide boundary layer might be due to a kind of local action cells. However, when attempts were made to observe local hydrogen gas evolution on the sulfide boundary by using an optical microscope, no gassing could be seen. Of course, it could be that the gas evolution rate was smaller than that necessary for bubble formation.

Also, thin cracks C appearing on the surface 1, and not visible on surface 2 probably are connected with the amorphous unstable structure of solid Cr at surface 1. It could be that the brittleness of Cr is at least partly due to the existence of these small cracks.

The surface roughness and surface profile analyses made by using AFM (see Figs. 7a,b and Fig. 8) also show that the amorphous surface is somewhat rougher (about 1.4 times), and for some reason, dissolves anodically (or corrodes) faster than the crystalline part of the electrode. It can be concluded that the crystalline structure and orientation has a certain influence on the rate of corrosion. However, a proper conclusion can only be made if a real single crystal Cr electrode were used for the experiments and if the experiments were made with surfaces oriented in a very defined manner. Attempts in this direction will be made in the future.

Acknowledgements: This work was financially supported by the Ministry of Science and Environmental Protection of the Republic of Serbia (Grant No. 1389) and the Serbian Academy of Sciences and Arts (Project F-7(4)). Thanks are also due to Professors Stevan Djurić and Pantelija Nikolić for providing premises and performing X-ray measurements as well as the fruitful discussion.

ИЗВОД

ЕЛЕКТРОХЕМИЈА АКТИВНОГ ХРОМА. ДЕО IV. РАСТВАРАЊЕ ХРОМА У ДЕАЕРИРАНОМ ВОДЕНОМ РАСТВОРУ СУМПОРНЕ КИСЕЛИНЕ

Д. М. ДРАЖИЋ¹, Ј. П. ПОПИЋ¹, Б. ЈЕГДИЋ² И Д. ВАСИЉЕВИЋ-РАДОВИЋ³

¹Институт за хемију, технологију и металургију – Центар за електрохемију, б. бр. 473, Њежишева 12, 11001 Београд, ²Војно-технички институт, Кашанићева 14, Београд и ³Институт за хемију, технологију и металургију – Центар за микроелектронске технологије и монокристале, Њежишева 12, 11000 Београд

Проучавано је анодно растварање хрома у воденим растворима сумпорне киселине у области рН 0,5 – 3 потенциостатском и врло спором потенциодинамичком методом, као и аналитичким праћењем промене концентрације Cr јона током експеримента. Показано је да електрохемијско анодно растварање прати уобичајено Тафелово понашање са нагибом Тафелове праве од око 120 mV dec⁻¹, као и да је независно од рН и хидродинамике. Међутим, потенцијали пасивације и струје пасивације такође су независни од хидродинамике, али врло зависне од рН. Једновремено са електрохемијским растварањем одиграва се и значајно "аномално" или хемијско растварање хрома. Ово је потврђено и спектрофотометријским анализама раствора током дужег потенциостатског одржавања катодних и анодних поларизација, као и мерењем губитка масе електроде. Сви ови резултати указују на одигравање независне реакције растварања хрома која није зависна од потенцијала, као што је случај са електрохемијском реакцијом. Предложени су механизми одигравања оба наведена процеса. Размотрене су и последице постојања оба наведена феномена на понашање неких практичних система у којима се користи хром или легуре хрома (нпр. нерђајући челик).

(Примљено 28. маја 2004)

REFERENCES

1. D. M. Dražić, J. P. Popić, *J. Serb. Chem. Soc.* **67** (2002) 777
2. G. T. Burstein, M. A. Kaerns, J. Woodward, *Nature* **301** (1983) 629
3. D. M. Dražić, J. P. Popić, *Corrosion* **60** (2004) 297

4. J. P. Popić, D. M. Dražić, *Electrochim. Acta* **49** (2004) 4877
5. R. M. Lazorenko-Manevich, A. N. Podobaev, *Zashch. Metal.* **37** (2001) 440
6. D. M. Dražić in *Modern Aspects of Electrochemistry*, Vol. 19, B. E. Conway, J. O' M. Bockris and R. E. White, Eds., Plenum Press, New York, 1989, p. 126
7. M. Pourbaix, *Atlas of Electrochemical Equilibria in Aqueous Solutions*, Pergamon Press, New York, 1966, p. 226
8. C. Wagner, W. Traud, *Z. Elektrochem.* **44** (1938) 391
9. Ya. M. Kolotyркин, *Z. Elektrohem.* **62** (1958) 664
10. Ya. M. Kolotyркин, G. M. Florianovich, *Zashch. Metal.* **1** (1965) 7
11. Ya. M. Kolotyркин, G. M. Florianovich, *Elektrokhimiya* **9** (1973) 988
12. Ya. M. Kolotyркин, G. M. Florianovich, *Glasnik Hem. Društva Beograd* **48** (1983) S125
13. Ya. M. Kolotyркин, T. R. Agladze, *Zashch. Metal.* **4** (1967) 413
14. Ya. M. Kolotyркин, G.M. Florianovich, *Zashch. Metal.* **30** (1984) 14
15. G. M. Florianovich, *Russ. J. Electrochem.* **36** (2000) 1037
16. T. Agladze, *Russ. J. Electrochem.* **36** (2002) 1057
17. W. J. James, in *Advances in Corrosion Science and Technology*, Vol. 4, M. G. Fontana, R. W. Staehle, Eds., Plenum Press, New York, 1974, p. 85.